A Simplified Constitutive Model for Reinforced Concrete Interfaces under Cyclic Loading

A. R. Moradi, M. Soltani M. & A. A. Tasnimi
Tarbiat Modares University, Tehran, Iran

SUMMARY:
Seismic response of RC structures primarily depends on the behavior of its members and structural interfaces. The nonlinear response of RC element is mainly due to concrete cracking, reinforcement plasticity and also their interaction. Stress transfer mechanism across cracks can be qualitatively classified as normal and shear stress. Reinforcement and concrete bond is put in the former while aggregate interlock and dowel action in the latter. The main objective of this paper is the simulation of RC cracks by developing the proper constitutive model for dowel action. This paper aims at developing a simplified model for crossing dowel bar based on the beam on elastic/inelastic foundation theory. Also a microphysics-based model developed by Li et al. is implemented and used to simulate the behavior of RC cracks and interfaces. Finally the constitutive verification of the model is carried out by comparing computational predictions with available experimental results.

Keywords: Dowel action, Shear, Cyclic loading, RC Crack

1. INTRODUCTION

Proper constitutive models can be an efficient tool to analyze RC structures under earthquake loading. Structural interfaces may be present in pre-formed joints, which are common in precast concrete, construction joints in cast-in-place concrete and stress-induced interfaces or cracks, which commonly occur in beam–column connections, brackets and corbels, etc. These interfaces may turn out to be critical planes in the operation of the load-resisting mechanism and govern the ultimate strength, ductility and energy absorption capability of an entire structure (Soltani and Maekawa, 2008).
Joints and interfaces are basic components of many RC structures. The behavior of RC cracks and interfaces is complex due to different types of stress transfer mechanism such as aggregate interlock and dowel action. Earthquake excitations will form localized damages at connections (e.g. beam-column) and increase crack opening during load reversals. Aggregate interlock deteriorates fast with crack widening. This makes dowel action as the main resisting mechanism at RC connections. On the other hand the dowel action is the only resisting mechanism at pre-formed joints, contraction connections and precast structures.

This paper aims at developing a constitutive model to simulate dowel action mechanism of deformed bar across RC cracks and interfaces. The model is based on the beam on the elastic foundation (BEF) and will be extended to the beam on inelastic foundation (BIF) by proposing an elasto-plastic formulation for subgrade stiffness. Contact density model proposed by Li et al. (Maekawa et al., 2003) is implemented to simulate aggregate interlock mechanism. The models are combined to compute the capacity of RC cracks under different types of loadings.

2. DOWEL ACTION

During the past years, extensive experimental and analytical investigations have been carried out to investigate the shear transfer behavior of dowel bars across cracks. Most investigators reported Beam on Elastic Foundation analogy (BEF) as a suitable tool to simulate the behavior of crossing bars. The first studies on the dowel action of the reinforcement were conducted on contraction joints in concrete highway pavement. The results from the contraction joint investigations, however, cannot be directly applied to other structural problems where significant nonlinear response as induced by concrete cracking and material nonlinearities, is observed (ASCE, 1982). Maekawa and Qureshi (Maekawa and Qureshi, 1996a) proposed a micro scale model for prediction of reinforcing bar behavior under the generic condition of axial pullout and transverse displacement. The formulation established by considering the combined axial pullout and transverse dowel action. Maekawa and Qureshi (Maekawa and Qureshi, 1996b) showed that coupling of pullout and transverse shear of steel at a crack cannot be ignored in structural analysis. Then, Maekawa and Qureshi (Maekawa and Qureshi, 1997) presented a unified model to simulate the behavior of interface transfer mechanism. Soltani and Maekawa (Soltani and Maekawa, 2008) extended the model proposed by Maekawa and Qureshi (Maekawa and Qureshi, 1996b) to path-dependent cyclic loading case. The model determines the deformational behavior of deformed bars by solving the nonlinear equilibrium and compatibility equations numerically with respect to the loading path and history. Since, they considered the crossing bar as a three-dimensional member capable of developing coupled shears and moment in addition to axial force, the model is time consuming.

In this paper, the BEF is extended to the BIF by proposing an elasto-plastic formulation for subgrade springs. The stiffness deformation relation ($k_s - \delta$) for springs is suggested based on studies conducted by Soltani and Maekawa (Soltani and Maekawa, 2008) and Maekawa and Qureshi (Maekawa and Qureshi, 1996b).

2.1. Monotonic loading

In spite of its shortcomings, the BEF analogy has been recognized as the most suitable approach to simulate concrete and reinforcement interaction, so called dowel action, across cracks and different types of connections in RC structures. Beam on elastic foundation is made of infinite similar elastic springs which connect a beam to an elastic subgrade. Dowel action mechanism is simulated by considering the crossing bar as a beam and the surrounding concrete as elastic foundation which is represented by springs. Each spring force is considered to be proportional to the corresponding deflection at the spring location (Fig. 2.1.1). Dowel shear carried by embedded bar can be determined from springs stiffness (k_s). The crossing bar at crack subjected to shear deformation can be treated as a semi-infinite beam resting on the elastic foundation. Hetenyi (Hetenyi, 1946) derived the required formulation by assuming elastic behavior for beam and foundation.

$$y(x) = \frac{2P\lambda}{k_s} D_{\lambda x} \tag{2.1.1}$$

$$\theta(x) = -\frac{2P\lambda^2}{k_s} A_{\lambda x} \tag{2.1.2}$$

$$M(x) = -\frac{P}{\lambda} B_{\lambda x} \tag{2.1.3}$$

$$V(x) = -P.C_{\lambda x} \tag{2.1.4}$$

$$\begin{aligned} A_{\lambda x} &= e^{-\lambda x}\left(\cos\lambda x + \sin\lambda x\right) \\ B_{\lambda x} &= e^{-\lambda x}.\sin\lambda x \\ C_{\lambda x} &= e^{-\lambda x}\left(\cos\lambda x - \sin\lambda x\right) \\ D_{\lambda x} &= e^{-\lambda x}.\cos\lambda x \end{aligned} \tag{2.1.5}$$

$$\lambda = \sqrt[4]{\frac{k_s}{4E_s.I_b}} \tag{2.1.6}$$

where $y(x), \theta(x), M(x), V(x)$ are deflection, rotation, moment and shear profiles of beam respectively. I_b is the moment of inertia of the bar and E_s is the elastic modulus of steel. Dowel shear is the amount of shear at the location of applied load ($x = 0$), so:

$$V_d(\delta) = \frac{k_s.\delta}{2\lambda} \rightarrow V_d(\delta) \propto [k_s(\delta)]^{3/4} \tag{2.1.7}$$

The above equation shows that the dowel shear directly depends on the applied shear displacement (δ) and material properties that is described by spring stiffness (surrounding concrete) and reinforcing bar. In fact, it can be used for all types of loading paths by adopting a proper formulation for spring stiffness. It is clear that at the early stages of loading, surrounding concrete response is elastic and Eqn. 2.1.7. has a fair accuracy. Increasing bar shear deformation leads to local crushing of the concrete under the embedded bar and separation of the subgrade can be occurred. Gradual changes in springs stiffness can be a convenient method to simulate the damages and fractures at the vicinity of shear plane.

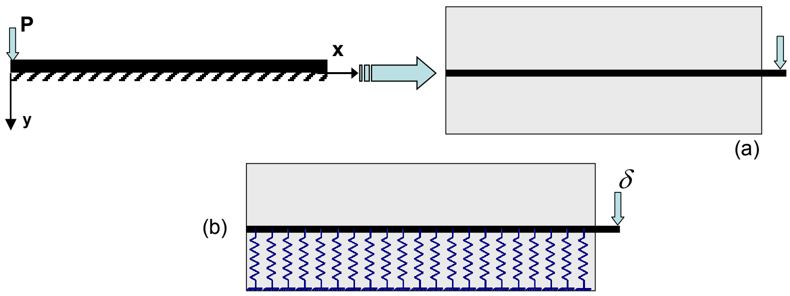

Figure 2.1.1. Dowel action simulation by using the BEF model, a) semi-infinite beam on elastic foundation, b) Equalizing with the BEF

In this paper in order to determine the behavior of springs and to propose a reasonable formulation for the stiffness of springs, dowel shear in Eqn. 2.1.7. is equalized with the model developed by Soltani and Maekawa (Soltani and Maekawa, 2008). To consider the effect of the localized curvature in the bar, close to the shear plane, the concept of a Curvature Influencing Zone, L_c, is introduced by Maekawa and Qureshi (Maekawa and Qureshi, 1996b). They experimentally evaluated the induced curvature of crossing bars under applied shear deformation. The shape of curvature profile, $\phi(x)$ within the zone (Fig. 2.1.1.) is considered as:

$$\phi(x) = \begin{cases} \dfrac{3.\phi_{\max}.(L_c - x)^2}{L_c^{\,2}} & , \dfrac{L_c}{2} \le x < L_c \\ \dfrac{-3.\phi_{\max}}{L_c^{\,2}} . \left[3.\left(\dfrac{L_c}{2} - x\right)^2 - L_c.\left(\dfrac{3}{4}.L_c - x\right) \right] & , 0 \le x < \dfrac{L_c}{2} \end{cases} \tag{2.1.8}$$

$$\phi_{\max} = \frac{64.\delta}{11 L_c^{\,2}} \tag{2.1.9}$$

Since dowel shear is defined as the amount of shear at the shear plane ($x = 0$), we focus on the first portion of the zone.

$$\phi(x) = -\frac{3\phi_{max}}{L_c^2}.\left[3\left(\frac{L_c}{2} - x\right)^2 - L_c.\left(\frac{3}{4}.L_c - x\right)\right],\ 0 \le x < \frac{L_c}{2} \tag{2.1.10}$$

When the applied shear deformation is too small, the bar and surrounding concrete remain elastic so L_c can be computed from the BEF analogy. The gradual cracks and damages in concrete due to increasing bar shear displacements (δ) are modeled by considering an increase in L_c as a function of initial value of L_{c0} by defining a non-dimensional damage index (DI) as follows:

$$L_{c0} = \frac{3\pi}{4}\sqrt[4]{\frac{4E_s I_b}{k_{fc}.d_b}} \tag{2.1.11}$$

$$k_{fc} = \frac{150 f_c'^{0.85}}{d_b} \tag{2.1.12}$$

$$DI = \frac{\delta}{d_b} \tag{2.1.13}$$

$$\begin{aligned} &L_c = L_{c0} \quad for\ DI \le 0.02 \\ &L_c = L_{c0}\left[1 + 3(DI - 0.02)^{0.8}\right] \quad for\ DI > 0.02 \end{aligned} \tag{2.1.14}$$

where d_b and f_c are bar diameter and concrete compressive strength, respectively. The reinforcing bar strain field can be determined. Also bending moment and shear distribution along the embedded reinforcing bar can be expressed:

$$\varepsilon(x, y) = \phi(x).y = \frac{192}{11}.\frac{\delta\ .x.(2L_c - 3x)y}{L_c^4} \tag{2.1.15}$$

$$\sigma(x, y) = \varepsilon(x, y).E_s = \frac{192}{11}.\frac{\delta.x.(2L_c - 3x)y}{L_c^4}.E_s \tag{2.1.16}$$

$$M(x) = 2\int_0^{\frac{d_b}{2}}\left(\sigma(x).y.\sqrt{d_b^2 - 4y^2}\right)dy = \frac{3\pi}{11}\frac{d_b^4.E_s.\delta.x(2L_c - 3x)}{L_c^4} \tag{2.1.17}$$

$$V(x) = \frac{d}{dx}\left(M(x)\right) = \frac{6\pi}{11}.\frac{d_b^4.E_s.\delta.(L_c - 3x)}{L_c^4} \tag{2.1.18}$$

where y is the local coordinate of bar cross section. Therefore, the shear force carried by crossing bar is directly calculated as:

$$V_d = V(x = 0) = \frac{6\pi}{11}.\frac{d_b^4.E_s.\delta}{L_c^3} = \frac{384}{11}.\frac{E_s.I_b.\delta}{L_c^3} \tag{2.1.19}$$

Eqn. 2.1.19. expresses dowel shear by assuming elastic response. By equalizing the simplified dowel action equation that is obtained from Soltani and Maekawa (Soltani and Maekawa, 2008) with Eqn. 2.1.4., the stiffness-deformation relation ($k_s - \delta$) of springs is obtained.

$$V\big|_{BEF} = V_d\big|_{Sol\tan i\&Maekawa} \tag{2.1.20}$$

$$x = 0 \rightarrow D_{\lambda x} = C_{\lambda x} = 1, P = \frac{\delta .k_s}{2\lambda} \tag{2.1.21}$$

$$\frac{384}{11} \cdot \frac{E_s.I_b.\delta}{L_c^3} = \frac{\delta.k_s}{2\lambda} \tag{2.1.22}$$

It can be rewritten as:

$$k_s(\delta) = 181\frac{E_s.I_b}{L_c^4} \tag{2.1.23}$$

by replacing Eqn. 2.1.13. and Eqn. 2.1.14. into Eqn. 2.1.23., the final form of the elasto-plastic formulation of spring stiffness is calculated.

$$k_s(\delta) = \begin{cases} 220 f_c^{0.85} & , \; DI \leq 0.02 \\ \dfrac{220 f_c^{0.85}}{\left[1 + 3(DI - 0.02)^{0.8}\right]^4}, & DI > 0.02 \end{cases} \tag{2.1.24}$$

Eqn. 2.1.24. shows that the foundation stiffness directly depends on the concrete compressive strength and the bar diameter indirectly. Elastic limit is defined by damage index parameter. The subgrade stiffness (k_s) is the most relevant parameter to capture the global behavior of embedded dowel bars hence by adopting the proper formulation, the final loading stage as well as the initial stage can be described. Local crushing and high inelasticity of surrounding concrete near the interface are simulated by gradual changes in the subgrade stiffness (Eqn. 2.1.24.) due to increasing bar shear displacements.

2.2. Cyclic loading

Dowel action mechanism has a considerable nonlinear response under reversed cyclic loading path. The source of nonlinearity should be sought in the plasticity of dowel bars and fracturing of the surrounding concrete. The amount of applied shear displacements as well as the direction of loading and also the number of loading cycles can lead to nonlinear response. To extend the formulation to unloading and reloading cases, we decompose the total displacement into two components, the elastic (δ_e) and the residual plastic (δ_p) displacements. Experimental observations show that unloading diagrams have relatively smooth form and can be expressed by a polynomial function with respect to the loading history (Soroushian et al., 1988 and Vintzeleou and Tassios, 1987). It seems that it is possible to predict the unloading curve by a parabolic function. In fact, shear-deformation formulation ($V_d - \delta$) can be derived just by two points (e.g. point A and B) for unloading curve.

According to Fig. 2.2.1., the load-deflection equation for unloading diagram can be expressed as:

$$V_d(\delta) = \frac{V_{d\max}.(\delta - \delta_p)^2}{(\delta_{\max} - \delta_p)^2} \tag{2.2.1}$$

where $V_{d\max}$ is the maximum dowel shear. Fig. 2.2.2. (b) shows the reliability of Eqn. 2.2.1. with respect to the available experimental data and the experimental program results for unloading stage ($\delta_p \leq \delta < \delta_{\max}$). The experimental values are normalized to compare in a consistent manner with the suggested equation. The embedded bar shear at each cycle is normalized by the maximum dowel shear and the elastic part is divided by the maximum shear slip.

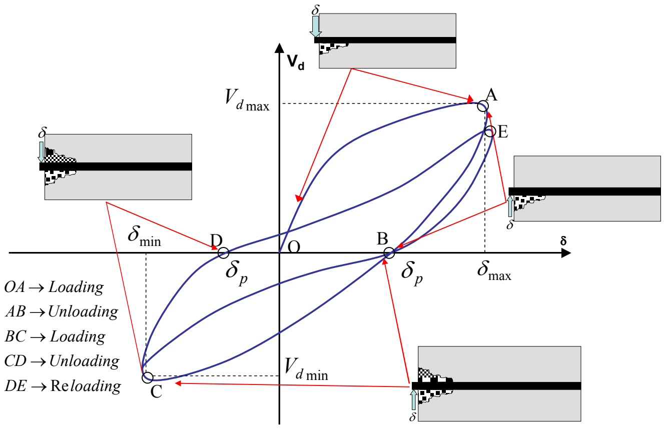

Figure 2.2.1. Schematic load-deflection dowel shear under reversed cyclic loading path

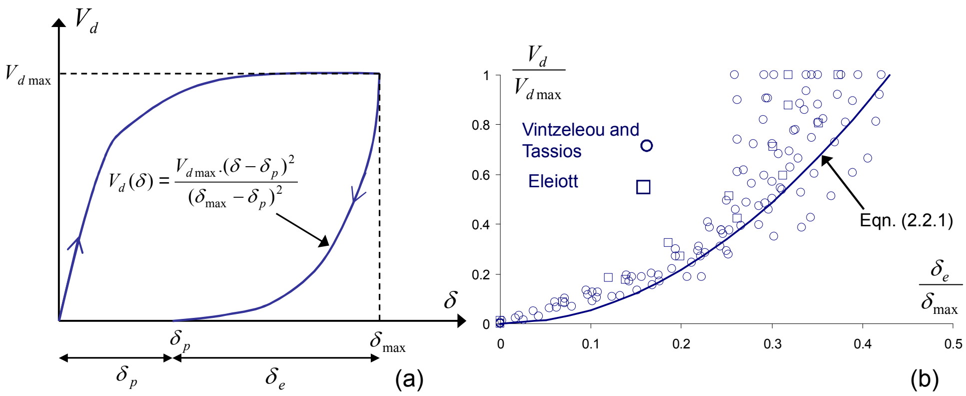

Figure 2.2.2. Determination of unloading diagram by a parabolic polynomial, a) equation derivation, b) comparison with the corresponding experimental results

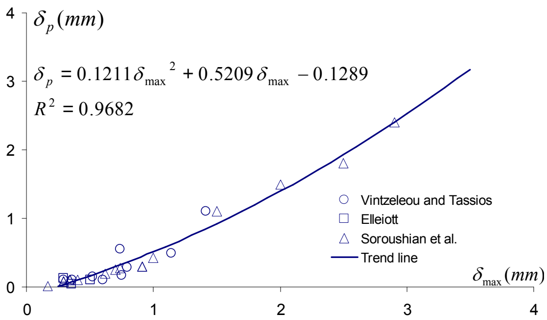

Figure 2.2.3. Regression of experimental results to determine the plastic displacement under cyclic loading

Experimental results show that the residual plastic displacement, δ_p changes due to increasing deformation of bar and cannot be assumed a constant value for it. Also it seems that determining the plastic bar displacement can improve the stiffness of unloading and reloading diagrams. So, the results of the available experimental results has been categorized for cyclic and repeating loading in order to obtain a reasonable relation between the maximum applied shear displacement, $\delta_{\max}$, and δ_p. The plastic displacement of dowel bar (δ_p) in each loading step is suggested by statistical analysis of the available experimental data and the experimental program results (Fig. 2.2.3.). The coefficient of correlation indicates the reliability of the proposed equations. The proposed equations (Fig. 2.2.3.) show that the plastic displacements under reversed cyclic and repeating loading depend on the maximum applied displacement and also cover the large applied shear displacements ($\delta_{\max} > 2mm$). The proposed formulation (Fig. 2.2.3.) will be adopted to extend the model to unloading and reloading cases.

3. MECHANISM OF SHEAR TRANSFER ACROSS RC CRACKS

Basically two main mechanisms of shear transfer across cracks are aggregate interlock (or shear friction) and dowel action due to the curvature of crossing bars at the RC interfaces. As the shear displacement path applies at the crack plane, overriding aggregates tend to widen the crack width (dilatancy). This crack opening increases the axial stress of bar while shear displacement causes flexure effect in bar. So, the overall stress state in reinforcing bar and surrounding concrete governs the crack opening and slip which can control the stress transfer across crack plane. It should be noted that the direct superposition of each formulation of aforementioned mechanisms (dowel action and aggregate interlock) cannot simulate the real behavior of RC interfaces. In Fig. 3.1. all mechanisms which affect the overall behavior of RC interfaces are shown. To determine the shear transfer across crack plane, the equilibrium of stresses at a crack can be written as:

$$\sigma = \frac{N}{A_c} + \rho\overline{\sigma}_s \tag{3.1}$$

where, ρ is the reinforcement ratio and N is externally applied force defined positive in compression. In fact by means of equilibrium (Eqn. 3.1.) it can be compute normal force due to aggregate interlock (σ) and the axial bar stress ($\overline{\sigma}_s$). σ is computed by contact density model (Maekawa et al., 2003). $\overline{\sigma}_s$ is calculated based on the explicit formulation proposed by Soltani and Maekawa (Soltani and Maekawa, 2008).

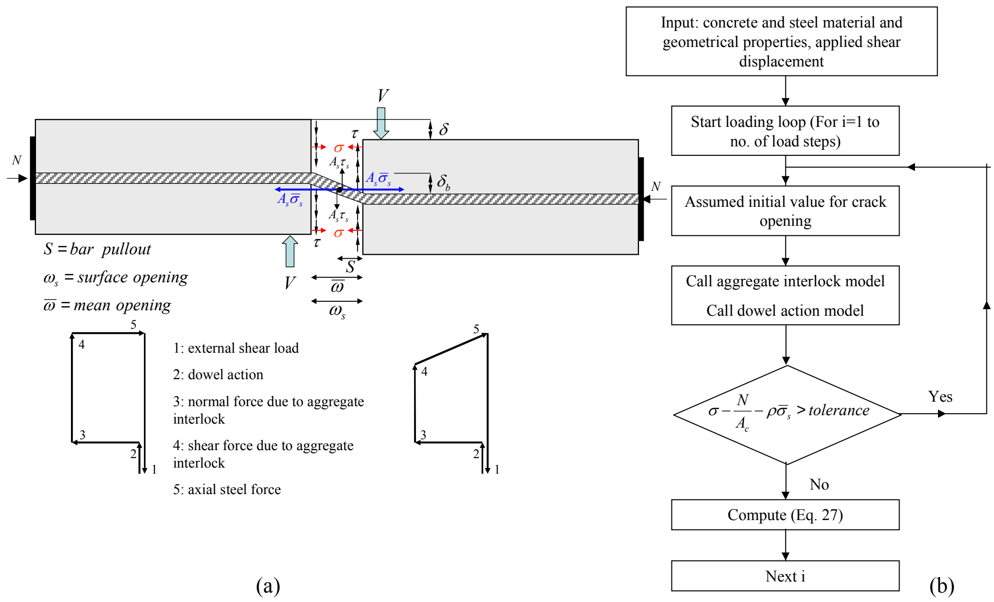

Figure 3.1. Shear transfer mechanisms across reinforced concrete crack, a) deformational and mechanical characteristics of a RC interface. The equilibrium condition for bars perpendicularly crossing the crack plane and for inclined bars crossing the crack plane, b) flowchart for the adopted method

Once the displacement paths (δ, ω) satisfy the equilibrium, the constitutive models for concrete shear (τ) and steel (τ_s) contribution determine corresponding mechanism and finally it can be computed the total shear transfer.

$$
\begin{aligned}
\tau_t &= \tau + \rho \tau_s \\
\tau &= \tau(\delta, \overline{\omega}) \\
\tau_s &= \tau_s(S, \delta_b)
\end{aligned}
\tag{3.2}
$$

The flow chart for solving (Eqn. 3.2.) across RC interfaces is shown in Fig. 3.1. Starting from assumed crack opening and adopting an iterative-based approach it can be satisfied the equilibrium. The only parameter that should be sought is the crack opening because shear displacement is known as input.

4. EXPERIMENTAL VERIFICATION

In order to verify the constitutive laws and check its applicability, some reliable experimental results are needed. Here we will verify dowel action and RC interface behavior under monotonic and cyclic loading.

4.1. Dowel action

To verify the proposed dowel action model, the experimental and computed dowel shear provided by different bar diameters under pure shear are shown in Fig. 4.1.1. Dei Poli et al. (Dei Poli et al., 1992) extensively investigated the behavior of dowel action. The comparison of the analysis and the experimental results are shown in Fig. 4.1.1. for different bar diameters. Satisfactory correlation can be observed for different specimens.

The experiment carried out by Vintzeleou and Tassios (Vintzeleou and Tassios, 1987) are used to examine the reliability of the proposed model and the current procedure under cyclic loading paths. The cyclic degradation of dowel shear stiffness is well simulated during load reversals. Good agreement between experimental and computed plastic residual is observed.

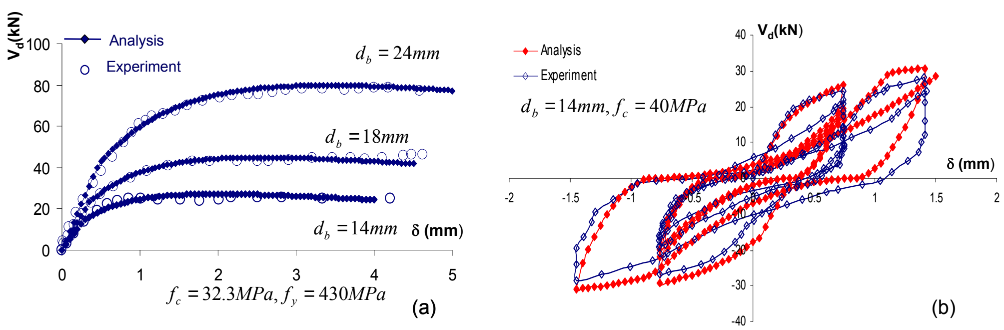

Figure 4.1.1. Comparison of test results and the model, a) comparison with test results reported in (Dei Poli et al., 1992) under monotonic loading, b) comparison with experimental results under reversed cyclic loading (Vintzeleou and Tassios, 1987)

4.2. Verification of stress transfer model

The accuracy and reliability of the proposed model (dowel action) and the developed algorithm (section 3) are examined through the corresponding experimental results to simulate the behavior of RC interfaces. Prediction for the behavior and the response of the RC cracks will be verified under monotonic and reversed cyclic loading path. For model validation, we use the results of experimental program which carried out by Maekawa and Qureshi (Maekawa and Qureshi, 1997) under monotonic loading path. They tested beam-type specimens and determined the contribution of each mechanism separately (Fig. 4.2.1.). In Fig. 4.2.1. τ, τ_d, τ_t denoted for aggregate interlock shear, shear due to dowel action and the total shear transfer across crack respectively.

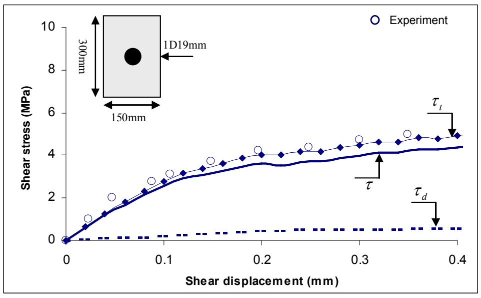

(a) $f'_c = 41.3MPa,\ \rho f_y = 2.76MPa,\ f_y = 389MPa$

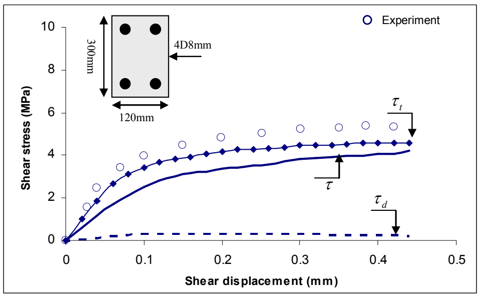

(b) $f'_c = 26.1MPa,\ \rho f_y = 2.58MPa,\ f_y = 460MPa$

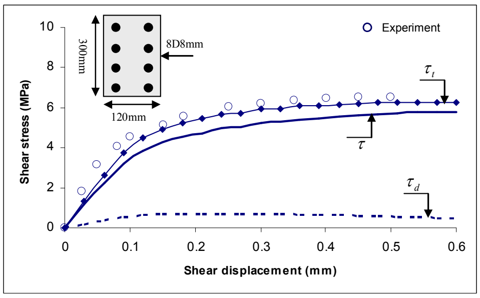

(c) $f'_c = 41.3MPa,\ \rho f_y = 5.15MPa,\ f_y = 389MPa$

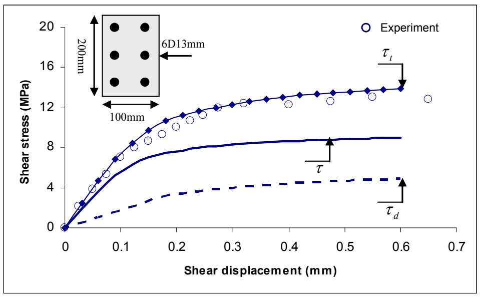

(d) $f'_c = 44.3MPa,\ \rho f_y = 14.3MPa,\ f_y = 376MPa$

Figure 4.2.1 Predicted and experimental shear stress-associated displacement relation at interface

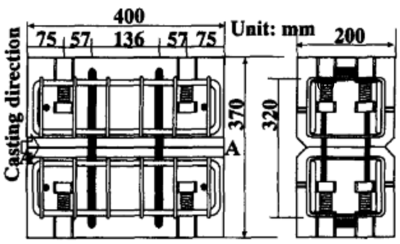

(a)

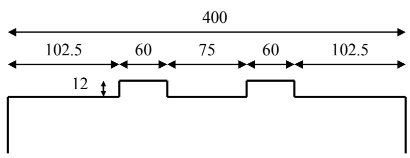

(b)

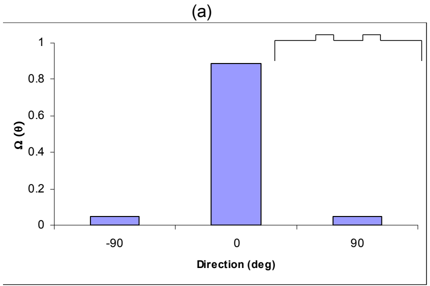

(c)

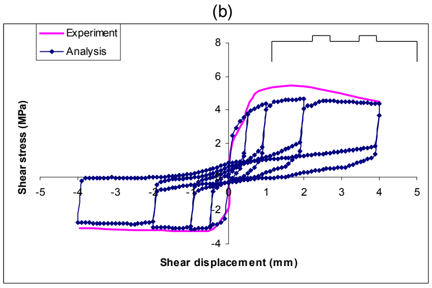

$d_b = 25mm, f_y = 386MPa, E_s = 184GPa, f_c = 44.1MPa$

(d)

Figure 4.2.2. Kono et al. experiment definition and verification, a) Dimension and reinforcement arrangement of the specimen, b) interface finishing for rectangular key type, c) histograms as contact density function for rectangular key interface, d) comparison with experimental result

Kono et al. (Kono et al., 2001) experimentally investigated the shear transfer at construction joints for high-strength and normal weight concrete. The results of this research are used to verify the applicability of the model under reversed cyclic loading. The most important feature of the research is the finishing of the RC interface. The specimens are made up of two blocks which the lower block was cast first (Fig. 4.2.2. a). The shear interface has specific kind of finishing as shown in Fig. 4.2.2. (b). One of the key inputs of the aggregate interlock model is the contact density function ($\Omega(\theta)$). Based on the experimental observations, Li et al. proposed $\Omega(\theta) = 0.5\cos(\theta)$ for normal weight concrete. But for this type of interface (Fig. 4.2.2. b), $\Omega(\theta)$ should be determined. Since for this interface and orientation angles (-90°, 0°, 90°), $\Omega(\theta)$ has a discrete form (histogram) as shown in Fig. 4.2.2. (c). According to the interface type that is shown in Fig. 4.2.2. (b), the corresponding histogram is determined in Fig. 4.2.2. (c) and defined as an input for the model.

It can be seen the results of analysis and the envelope curve for experimental result in Fig. 4.2.2. (d) under cyclic displacement path. Despite of the finishing form, the cyclic degradation and ultimate shear strength are well simulated by the model.

5. CONCLUSION

A macro scale constitutive model for dowel action mechanism was proposed to simulate the behavior of deformed bar across RC cracks. Explicit formulation of the BEF showed that dowel deformational profiles ($y(x), \theta(x), M(x), V(x)$) can be simply determined. Also the model was developed to capture the reversed cyclic loading path. The cyclic deterioration was considered in a consistent manner.

The proposed model for dowel action and contact density model proposed by Li et al. (Maekawa et al., 2003) were implemented to simulate the response of different types of RC cracks and interfaces under monotonic and cyclic loading paths. The reliability and the accuracy of the model were examined by comparing with experimental observations under monotonic and cyclic loading. The results showed that the current model can simulate the response of RC connections (e.g. beam-column) during seismic excitations and can be a proper tool in assessing the capacity of RC members.

REFERENCES

ASCE Task Committee on Finite Element Analysis of Reinforced Concrete Structures, (1982). State-of-the-Art Report on Finite Element Analysis of Reinforced Concrete. New York, ASCE.

Dei Poli, S., Di Prisco, M. and Gambarova, P. G. (1992). Shear response, deformation, and subgrade stiffness of a dowel bar embedded in concrete. *ACI Structural Journal.* **89:6**,665-675.

Hetenyi, M. I. (1946). Beams on elastic foundation: Theory with applications in the fields of Civil and Mechanical Engineering, The University of Michigan Press.

Kono, S., Tanaka, H., Watanabe, F. (2001). Interface shear transfer for high strength concrete and high strength shear friction reinforcement. *Proceedings of International Conference on High Performance Materials in Bridges*. **28**:319-328.

Maekawa, K., Qureshi, J. (1996). Embedded bar behavior in concrete under combined axial pullout and transverse displacement. *Proceeding of JSCE.* **30:532**,183-195.

Maekawa, K., Qureshi, J. (1996). Computational Model for Reinforcing Bar Embedded in Concrete under Combined Axial Pullout and Transverse Displacement. *Proceeding of JSCE.* **31:538**,227-239.

Maekawa, K., Qureshi, J. (1997). Stress transfer across interface in reinforced concrete due to aggregate interlock and dowel action. *Proceeding of JSCE.* **34:557**,159-177.

Maekawa, K., Pimanmas, A., Okamura, H. (2003). Nonlinear mechanics of reinforced concrete, SPON Press.

Soltani, M., Maekawa, K. (2008). Path-dependent mechanical model for deformed reinforcing bars at RC interface under coupled cyclic shear and pullout tension. *Engineering Structures.* **30:4**,1079-1091.

Soroushian, P., Obaseki, K., Baiyasi, M. I., El-Sweidan, B. and Choi, K. (1988). Inelastic cyclic behavior of dowel bars. *ACI Structural Journal.* **85:1**,23-29.

Vintzeleou, E. N., Tassios, T. P. (1987). Behavior of dowels under cyclic deformations. *ACI Structural Journal.* **84:1**,18-30.